INTERFACE

Research

Check for updates

Author for correspondence:
Loïc Tadrist
e-mail: loic.tadrist@uliege.be

THE ROYAL SOCIETY
PUBLISHING

Foliage motion under wind, from leaf flutter to branch buffeting

Loïc Tadrist[1,2], Marc Saudreau[2], Pascal Hémon[1], Xavier Amandolese[1], André Marquier[2], Tristan Leclercq[1] and Emmanuel de Langre[1]

[1]Laboratoire d'hydrodynamique, CNRS, École Polytechnique, 91128 Palaiseau, France
[2]INRA, Physique et physiologie intégratives de l'arbre fruitier et forestier, 63100 Clermont-Ferrand, France

(iD) LT, 0000-0001-6200-9842; TL, 0000-0002-5995-3354

The wind-induced motion of the foliage in a tree is an important phenomenon both for biological issues (photosynthesis, pathogens development or herbivory) and for more subtle effects such as on wi-fi transmission or animal communication. Such foliage motion results from a combination of the motion of the branches that support the leaves, and of the motion of the leaves relative to the branches. Individual leaf dynamics relative to the branch, and branch dynamics have usually been studied separately. Here, in an experimental study on a whole tree in a large-scale wind tunnel, we present the first empirical evidence that foliage motion is actually dominated by individual leaf flutter at low wind velocities, and by branch turbulence buffeting responses at higher velocities. The transition between the two regimes is related to a weak dependence of leaf flutter on wind velocity, while branch turbulent buffeting is strongly dependent on it. Quantitative comparisons with existing engineering-based models of leaf and branch motion confirm the prevalence of these two mechanisms. Simultaneous measurements of the wind-induced drag on the tree and of the light interception by the foliage show the role of an additional mechanism, reconfiguration, whereby leaves bend and overlap, limiting individual leaf flutter. We then discuss the consequences of these findings on the role of wind-mediated phenomena.

1. Introduction

Plants move under wind, as is shown by common experience. These movements have been long observed, and even used as indirect measurement of the wind magnitude. Still, they were often thought to be of minor importance for the plant itself, provided that they did not cause breakage or uprooting. In fact, most of the past research on wind–plant interaction focused on the fatal risk that wind might cause to the living plant [1,2]. But wind does affect plants even in lower wind levels by several ways. Even without considering wind-induced motion, wind plays a key role in the thermal state of the plant [3,4], and in gaseous exchanges and transports [5,6]. These two factors are of the utmost importance in photosynthesis, the motor of plant life [7].

The indirect role of wind on plant life, through wind-induced motions, is even more diverse, see for instance the review in [1]. Photosynthesis, mentioned above, is also directly affected by leaf motion [8,9] that alters light interception [10] and the airflow boundary layer [5] and, thereby, the thermal exchange scheme.

It is also now known that deformations such as those induced by wind, are perceived by plants, resulting in changes in the growth, more particularly in biomass allocation [11]. But motion is also a dominant factor in seed or pollen ejection, thereby affecting plant reproduction [12,13]. Motion also affects the duration of water retention on leaves, a key factor in pathogen development, and conversely, the capture of pesticides [14–16].

More generally, moving leaves or branches also affect the presence of insects, and even the damage caused by herbivores [17,18]. Even wi-fi

transmissions have been found to be affected by the motion of leaves [19,20]. Recent evidence has shown that wind-induced plant motion can even affect the gestural language of chimps in forest environments [21], or communication between lizards [22].

Finally, the perception by humans of wind-induced motion of plants is now being explored *per se*, in the realm of video games and animation films [23]. Good rendering of plant motion is a key to realistic outdoor scenes, as plants are the most common outdoor flexible structures. However, the computational time required to simulate a moving tree remains important because of the different length and timescales present in a tree [24]. Solutions using lower computational resources like hybrid model merging physical simulation and random tuned turbulence [25] or direct motion capture for tree animation [26] are explored.

To summarize, understanding the wind-induced motion of plants is of interest in many fields of plant science, agronomy, biology and engineering. For instance, in biology, it is essential to understand how trees extract energy from their windy environment [9], in agronomy, it is essential to understand how foliage motion may improve the efficiency of pesticide spreading [15] and finally in computer science, it is essential to make realistic outdoor scenes using low computational resources [25].

Some distinctions need now to be made on the plant system that is considered. Differences may be made on the plant itself (yearly or not, large or small), but also between canopies and isolated plants. Canopies under wind have been mostly studied for application in crop science [27–31]: wheat, rice, alfalfa, for instance, do move under wind, but more as a continuous medium than as individuals. Conversely trees are more generally considered as individuals [32–35], whether isolated or in forest canopies. But, more importantly, they generally have an architecture that is far more complex than most crops [36]. This appears clearly when considering the successive levels of branching, from the trunk to the smallest twigs and the resulting number of branches. The number of leaves is also very large, up to 10^5. We shall focus now on trees, in the sense of a system made of branches that hold a large number of leaves.

When considering the wind-induced motion in a tree, two scales are generally considered [1,2]. The first is the large scale, corresponding to the global swaying of the tree or branches, and the second, a much smaller one, when a leaf flutters by itself. Most of the past work on trees has focused on these two extreme scales, the full tree [35,37–42] or the individual leaf on a fixed branch [4,5,43–45]. But many of the effects mentioned above need to be considered at the level of the whole foliage, defined here as the full set of leaves, considered statistically [46–48]. When considering the absolute motion of the foliage, it seems to be a combination of the small scale motion of the leaves relative to the branches they are attached to, and the large scale motions of these branches. There is clearly a need to decipher what governs total foliage dynamics.

Although models exist for leaf or branch dynamics under wind, see for instance in Gardiner *et al.* [2], no experimental or analytical work has considered the whole foliage of a tree as a continuous dynamic medium. Recent work has shown that optical measurement and powerful data processing allow the extraction of important features from the dynamics of complex plants systems [49–51]. Moreover, we have

shown recently that it is possible to incorporate wind effects on the statistics of leaf orientation, for light interception [48]. In this paper, we aim to clarify the relative contribution of leaves and branches in the dynamics of the foliage as a whole. For this, we consider a simple enough system, a small young tree, in a controlled wind environment, a large-scale wind tunnel, using several independent types of measurements: drag force, light interception and foliage motion. A comparison with existing models is presented to give a consistent view of the evolution of the foliage dynamics under wind. The possible outcomes of this work are discussed in §5.

2. Material and methods

A young cherry tree, *Prunus Cerasus*, is placed in a wind tunnel, figure 1. Technical details on the material and methods of the experiments are given in the corresponding appendix. The view of the tree is essentially that of the foliage, due to the foliage density. It has a simple architecture with a main rigid trunk and straight flexible branches holding leaves. Its main characteristics are summarized in table 1. Tests in the absence of wind enabled the derivation of the main mechanical and geometrical characteristics of the tree, of the branches and of the leaves. In the wind tunnel, an airflow is generated and maintained for several minutes at prescribed values of mean flow velocity, between 1 and about $8 \, \mathrm{m \, s^{-1}}$. Note that these are rather low wind intensities when compared with other tests aimed at the bending and fracture of trees [39,41,42].

Several types of measurements were made on the tree under a given wind speed. First, forces and moments at the base of the tree were measured with a load cell, and averaged over time at a given wind velocity. Additional tests on wind loads on the trunk only, after cutting all branches, and elementary force and moment reconstruction allowed derivation of the drag on the tree crown only. This will be referred to as the drag hereafter. Second, using a camera placed on the floor of the wind tunnel, the light intercepted by the tree was recorded. The relevant quantity is the normalized light interception, I, defined here as the fraction of sky occupied by leaves and properly time averaged. Finally, a lateral view of foliage motion was recorded using a fast camera. The local instantaneous velocity field of the foliage, $v(x, t)$, was estimated using a tracking method, which has been shown previously to be particularly adapted for the measurement of motion in plants [50,51]. The local variance in time was then space-averaged over the whole surface occupied by the tree in the picture frame. For each level of the wind velocity, U, we then have an apparent total foliage velocity, V, defined as,

$$V = \sqrt{\langle \langle v^2 \rangle_t - \langle v \rangle_t^2 \rangle_x}, \qquad (2.1)$$

where $\langle \ \rangle_t$ and $\langle \ \rangle_x$ stand for time and space averaging, respectively. We also seek to separate the respective contributions of the branch-induced motion and of the leaf motion relative to the branch in the total foliage motion. To do so, the original velocity field, $v(x, t)$, is decomposed using a bi-orthogonal decomposition, as in [34,52,53]. We then separate these modes in two groups, based on the size of the part of the foliage moving in each mode: local (leaf-size) modes and global (branch-size) modes of motion (see appendix A for details). These two groups will then be used to reconstruct the total foliage velocity V as the sum of a global ('branch-induced' or 'branch') velocity and a local (leaf) velocity,

$$V^2 = V_\mathrm{b}^2 + V_\mathrm{l}^2, \qquad (2.2)$$

where V_b and V_l stand for the branch and leaf velocities, respectively.
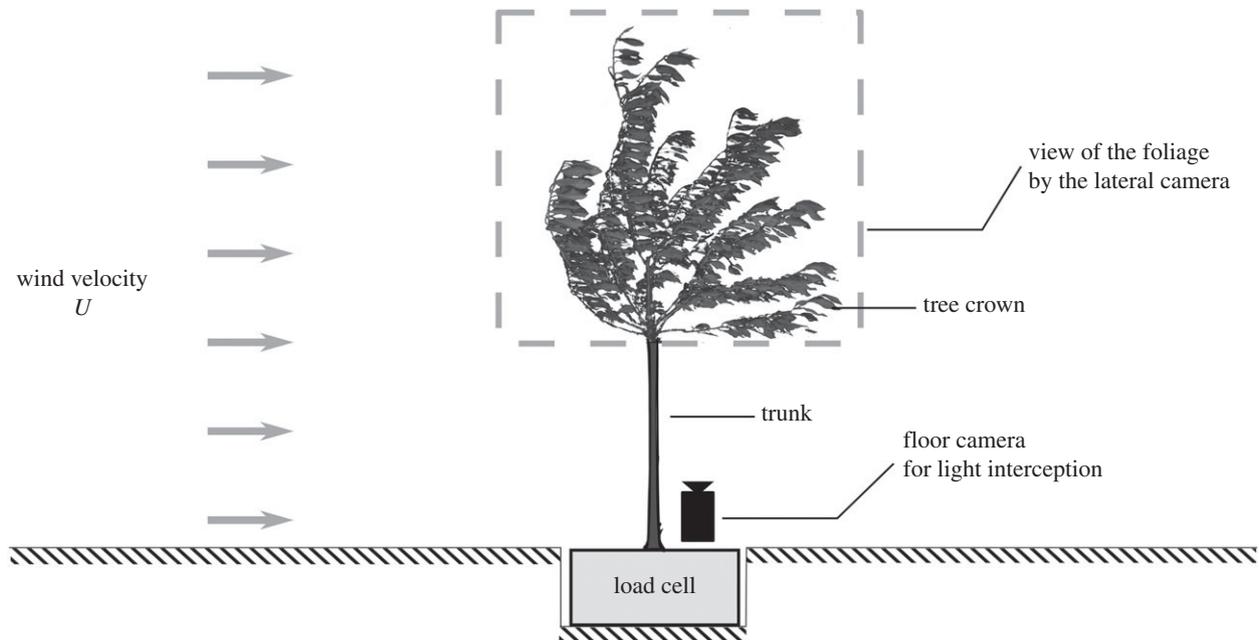
Figure 1. Schematic view of the experiment.

Table 1. Mechanical and geometrical characteristics of the cherry tree used in the experiment.

trunk	
diameter	57 ± 1 mm
branches	
number of branches	12
diameter	14.5 ± 5.5 mm
leaves per branch	143 ± 105
leaves	
number of leaves	1713
lamina length	99.1 ± 29.7 mm
lamina width	53.5 ± 9.1 mm
petiole length	39.0 ± 8.7 mm
mass	1.08 ± 0.65 g
torsional damping	0.034 ± 0.006
torsional frequency	6 ± 1 Hz

3. Results

We now present the results of the global measurements on the tree as a function of the wind velocity. The light interception I, figure 2a, is found to decrease regularly with the wind velocity. This corresponds to a reorientation of the leaves and branches that progressively overlap as is illustrated by the two inserts of instantaneous view by the camera. Simultaneously the drag on the tree crown, D, figure 2b, has a regular evolution with the wind velocity, but it is seen to deviate from the classical quadratic dependence on the velocity as it will be discussed later. For the foliage velocity V, figure 2c, several features need to be noted on the evolution. First, V increases only by a factor of about 4 when wind velocity is increased from 1 to $8 \, \mathrm{m \, s}^{-1}$. This is a much weaker dependence than currently observed in wind engineering of man-made structure [54]. Second, above about $3 \, \mathrm{m \, s}^{-1}$, the evolution appears to be irregular and marginal.

To separate the respective contributions of the motion of the branches and of the relative motions of the leaves, the bi-orthogonal decomposition as defined above is now used on the foliage velocity field $v(x, t)$. The modes resulting from the decomposition are characterized by their *topos*, which identify where the motion is spatially correlated for this mode and their *chronos*, which give the corresponding evolution in time. They may be separated in two groups, after removing artificial optical modes: (a) modes with both a wide spatial support and a low frequency time evolution; (b) modes with a more localized spatial support and a higher frequency time evolution. Typical modes from these two groups are illustrated figure 3a. The large scale motion, in blue, corresponds to the swaying of a whole branch, while the small scale motion, in orange, is more at the leaf scale.

Using this set of modes, we may now reconstruct the specific contribution of the leaf modes to the foliage motion V_1 by summing over all leaf modes, and similarly, the contribution of the branches V_b. In figure 3b, we show the evolution of these two quantities with the wind velocity, and their relative contributions in comparison with the total foliage velocity V. Surprisingly, very different evolutions are observed with the wind velocity: the large scale, branch-induced motion is found to be negligible at low wind, but increases steadily with the wind velocity and eventually becomes dominant above about $5 \, \mathrm{m \, s}^{-1}$. Conversely, the small scale leaf-induced motion dominates at low velocity, but with a small dependency on the wind velocity, and eventually even decreases above $3 \, \mathrm{m \, s}^{-1}$, with a more erratic evolution. Clearly, two different mechanisms of fluid–structure interactions are present here, and contribute to the foliage motion. We now seek to identify these two mechanisms and relate them to models.

4. Modelling foliage dynamics

Figure 3b shows that the part of the foliage motion due to branch motion had a rather regular evolution of its magnitude with wind velocity. Considering the large variety of
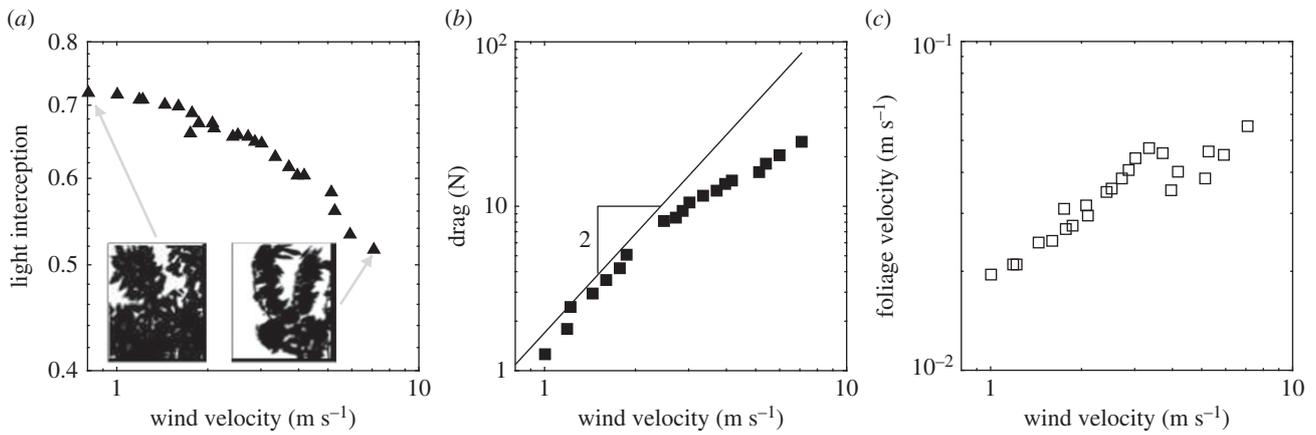
Figure 2. Global measurements on the tree as a function of the wind velocity U. (a) Light interception I, with instantaneous views from the camera (inserts), (b) drag on the tree crown D, in comparison with a quadratic dependence on velocity (rigid body), (c) foliage velocity V as defined in equation (2.1).
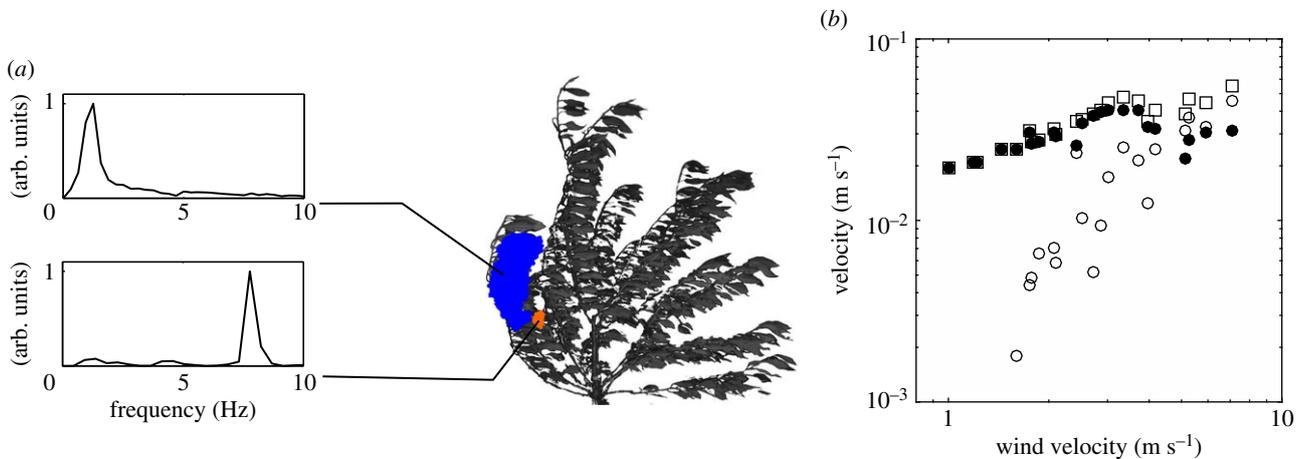

Figure 3. Bi-orthogonal decomposition of the foliage velocity. (a) Example of local (leaf) and global (branch) modes. The inserts show the corresponding PSD of the *chronos*. The branch mode has a *topos*, in blue, spanning over a large distance with a low frequency content (about 1 Hz). The leaf mode, in orange has a more localized *topos* and a higher frequency *chronos* PSD (about 8 Hz). (b) Total foliage velocity, V ($\square$), Leaves velocity, V_l ($\bullet$), branches velocity, V_b ($\circ$). (Online version in colour.)

possible fluid–structure interaction mechanisms that exist [55,56], this suggests that it results from the simple elastic response of the branches to wind turbulence, often referred to as the turbulent buffeting response. To test this assumption, we derive now the scaling of the dependence to the wind velocity that can be expected from this mechanism using standard methods [55]. A first step is to model the spectrum of fluctuating velocities. Although turbulence spectra in the wind tunnel may differ slightly from outdoor wind spectra, we use a typical von Kàrmàn spectrum [57], with a characteristic length of the scale of a metre. The typical frequency of motion of the branch modes being of the order of 1 Hz, the reduced von Kàrmàn frequency is larger than 0.1 as long as $U < 10\,\mathrm{m\,s^{-1}}$. In those conditions, the autocorrelation spectrum of velocity fluctuations, S_u, scales as $U^{8/3}$ [57]. The amplitude of vibration of an elastic medium to such fluctuations, considering the flow induced damping, scales as $U^{11/6}$ (see appendix B). Figure 4a shows that the part of the observed motion due to branches has a dependence on the wind velocity with a slope that is compatible with this elementary model. We may conclude that the part of the foliage motion due to large scale, coherent, low-frequency branch motion is here most probably due to the elastic response of foliage to the wind turbulence.

For locally correlated motions, a very different evolution is observed, and recalled in figure 4b. As noted above, the evolution of the leaf motion is here weakly dependent on the wind velocity. This small dependence with the flow velocity suggests that turbulence buffeting does not play any role. An alternative fluid–structure interaction mechanism, torsion flutter, has recently been shown to exist in leaves [45]. Contrary to turbulent buffeting it results, for a given leaf, in a sudden increase of oscillations once a critical velocity is reached. This critical velocity can be estimated based on the geometry and mechanical characteristic of the leaf, and its inclination with regards to the wind, see Tadrist *et al.* [45]. Using data measured on the leaves, table 1, a critical velocity can be estimated here at $U_c = 1.35\,\mathrm{m\,s^{-1}}$. This is the lowest velocity from which a leaf of the foliage is expected to flutter, see appendix B. For leaves with other orientations, the velocity from which flutter starts is higher, but as noted in Tadrist *et al.* [45] a large majority of the leaves will flutter for wind velocities at 50% above this critical velocity. Moreover, tests on individual leaves in a wind tunnel showed that for a fluttering leaf the amplitude of motion reached a limit value at about 30% above critical velocity. Hence, we expect that the part of the foliage velocity due to leaf flutter will start at about $1.35\,\mathrm{m\,s^{-1}}$, increase regularly as more and more
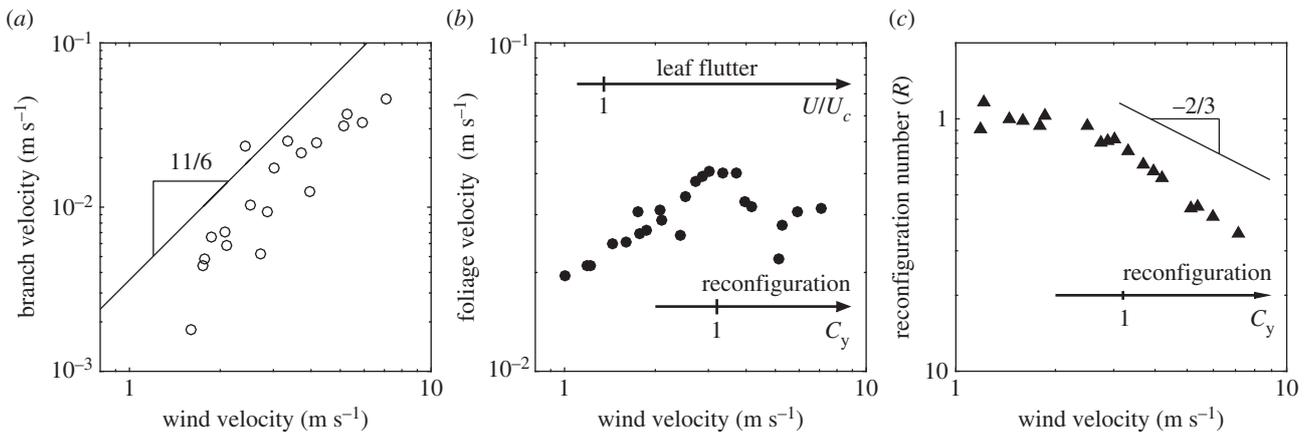
Figure 4. (a) Part of the foliage motion due to branch motion. ($\circ$) Experimental data, ($-$) scaling law using a standard model of turbulent buffeting. (b) Part of the foliage motion due to leaf flutter. The value of $U/U_c = 1$ in the scales corresponds to the predicted onset of leaf flutter. The value of $C_y = 1$ corresponds to the onset of significant change of orientation of leaves, called reconfiguration. (c) Reconfiguration number based on the drag measurement on the whole tree. The line corresponds to the scaling predicted by theory [59]. Reconfiguration is found above $C_y = 1$, as predicted.

leaves flutter and as each leaf reaches its limit cycle. Saturation of the level of foliage motion due to torsion flutter is expected at about $2.6 \, \text{m s}^{-1}$. This is fully compatible with the observation of a large amplitude of motion for small velocities and a weak dependence on wind velocity.

To understand the more erratic evolution of the leaf-induced motion above $3 \, \text{m s}^{-1}$, closer attention needs to be paid to the measured light interception I and drag D. As noted above, light interception, which is an indirect measure of the average deformation of the foliage is strongly modified by the wind velocity (figure 2a). Leaves are observed to progressively reorient and even overlap at the highest velocities, resulting in a decrease of light interception from 0.7 at rest to 0.5 with the highest wind. This is expected to alter their ability to flutter, because of contact between leaves. Another indirect measure of this static deformation of the leaves is seen on the evolution of drag on the tree, figure 2b. If the leaves were undeformed, the drag would be expected to grow as U^2, as on any system at high Reynolds number. We have noted that its evolution is not always quadratic with the wind velocity. This is a common feature of drag over flexible bodies, called the reconfiguration effect [58], and has been abundantly documented for plants, see for instance in [2,59–61]. To characterize this, the appropriate dimensionless number is the reconfiguration number R, defined as the measured drag referenced to the drag on the body if it did not deform. While the former is measured, the latter is usually extrapolated from measures of drag at velocities where the object of interest does not deform. A reconfiguration number lower than one implies a drag reduction due to flexibility. In figure 4c, the reconfiguration number deduced from the data of figure 2c is shown as a function of the wind velocity. Clearly, a change of regimes appears above about $2 \, \text{m s}^{-1}$. As most of the drag on the tree comes from the leaves, this change of drag regime is a sign that leaves have significantly deformed under wind. This is compatible with the previous observation, through the value of the light interception. The threshold for this reconfiguration is known to be related to the value of the Cauchy number [1,59, 62,63] which scales the fluid loading to the flexibility of a deformable body. The critical value of $C_y = 1$ would be reached at about $U = 3.2 \, \text{m s}^{-1}$, using the data from table 1 and from [48], see appendix B. The Cauchy axis is reported in figure 4b,c, and the onset of reconfiguration at $C_y = 1$ is

compatible with the change of regime. Moreover, the slope of the decrease in drag predicted by the theory, $U^{-2/3}$ [59], is also compatible with the data. This further confirms that a very significant static deformation of the leaves exist above a few metres per second. In terms of foliage velocity caused by leaf motion, this additional mechanism limits also the motion of the leaves, in a more erratic way as the leaves progressively bend, then overlap and clump together.

To summarize, we may now state that the motion of the foliage, as observed in our experiments, is the combination of branch motion due to turbulent buffeting with leaf torsion flutter, eventually altered by leaf deformation and overlapping at higher velocities. More generally, we expect that foliage motion under wind will be dominated at low velocity by high frequency, large amplitude, velocity independent individual leaf motions, and at high velocity by branch-induced, large scale, velocity-dependent motion.

5. Discussion

The main finding of this work is that two distinct mechanisms contribute to the motion of the foliage, at low or at high velocities. The cross-over between leaf-dominated motion and branch-dominated motion occurred, in our experiment, at a few metres per second. The upper limit of $8 \, \text{m s}^{-1}$ used here corresponds to a strongly deformed foliage, and is somehow the upper limit of foliage motion for that tree. The lower limit of $1 \, \text{m s}^{-1}$ is typically the velocity at which plants start to move. An analysis in terms of flutter critical velocity and Cauchy number would be necessary to adapt those limits to other trees. The tree we used in this experiment was chosen for its simple structure, both in terms of architecture (a single level of branching) and of foliage (homogeneous leaf characteristics and implantation in the tree). Its foliage was found, using [45], to be of simple mechanical behaviour. However, this tree has undergone significant artificial selection as it is used to produce cherries but we do not expect that this tree has been artificially selected according to its ability to flutter or resist winds and we do not consider that this tree is specifically representative of a larger population. Nevertheless, we expect that the two mechanisms we identified will be present in the response of most of the trees with leaves.

The remaining question is how the characteristics of a given tree play a role in the relative contribution of each of the two. We focus here on the geometrical characteristics, comparing small trees and tall trees, with small leaves or large leaves. To do so we explore how the foliage velocity at a given wind velocity would change if all geometrical characteristics were scaled by the same factor β, see appendix B for the following derivations. Leaf flutter only depends on the local characteristics of the leaves. The level of leaf-related foliage velocity would scale as β^0 and therefore not depend on the size of the leaves. Branch turbulence buffeting has a more complex dependence on the characteristics of a tree. If all lengths are scaled by a factor β, the velocity at a given wind velocity is found to vary as $\beta^{-1/2}$, which is a very weak dependence. On the axis of the wind velocity, the critical values will not change much either: the critical velocity for flutter U_c, see equation (B 4), scales as β^0: large or small leaves start to flutter at the same wind velocity. The elastic reconfiguration, controlled by the Cauchy number will not be dependent on the geometrical scales, as C_y, equation (B 6) varies as β^0. Finer allometry models might be taken into account but are not expected to change these scaling significantly, see for instance in Rodriguez et al. [64]. By this, we may infer that we expect the behaviour observed for our small tree to exist over a wide range of sizes of trees: first leaf flutter then branch buffeting above a few metres per second. As a conclusion, we may state that the behaviour of the foliage observed in this experiment would probably be found similarly in larger trees with larger leaves. Of course, varying independently the size of the leaves and of the tree and branches is feasible, with the models used here. But, again, as all quantities are weakly dependent on size, the relative contribution of leaves and branches to foliage motion is not expected to be much altered.

The experiment presented here, and the models we used, were not designed to study all the geometrical and mechanical factors that may play a significant role in the dynamics of various kinds of foliage. Some questions remain completely open. For instance, the dense foliage of a larger tree will have a motion that is certainly not uniform: the wind velocity will be lower inside the tree volume, but with a higher level of fluctuations [65]. The respective contributions of flutter and of turbulent buffeting might be different. Similarly, a larger tree with a higher level of branching is known to have a richer branch dynamics [64], which will result in a wider contribution of the branches in the dynamics of the foliage. This might also permit efficient damping (nonlinear transfer of energy) from the trunk and large branches to smaller branches and twigs [66]. Torsion flutter may also not be the only fluid–structure interaction mechanism at the leaf scale: for some leaves, coupled-mode flutter or vortex-induced vibrations [67] may contribute to the foliage motion. More generally, a noticeable variability exists inside a given tree, between individuals or among species on the geometries and material characteristics of all the components of the plant, from the leaf thickness to the angle of branching that affect foliage dynamics, according to the models we used here.

In all this work, we have considered the velocity of the foliage as the quantity of interest for the foliage dynamics. When referring to the numerous fields of applications mentioned in the introduction, finer analysis is needed to state whether foliage displacement, velocity or acceleration should be considered. Velocity is probably the quantity of interest for visual perception (human, animal) [24–26] and

wi-fi interception [19,20]. The decoupling between large scale motions and small scale motions, as suggested for realism in Selino & Jones [25], and experimentally shown here may be sound foundations for making realist virtual scenes in computer science. For water or insect retention, models of separation will rely on the acceleration of the foliage [16–18]. Acceleration, in our oscillatory motions, scales essentially as the velocity times the frequency of oscillation. We found that the local, leaf-size modes had a frequency of oscillation that was much larger than that of the global branch-size bending mode. Hence, the level of acceleration of the foliage is expected to be even more dominated by leaf flutter than for foliage velocity. Branch induced acceleration would require significantly higher winds. As a consequence, models of water or insect retention need only to take into account the motion of the leaves relative to the branches, not whole foliage motion. Conversely light capture by a given leaf depends on the change of orientation of the leaf, and therefore on foliage displacement rather than on velocity. As displacements scale as velocities divided by the frequencies, the role of branch motion might then become dominant.

Our experimental results, and their comparison with simple engineering-based models, show for the first time that the global motion of foliage is the combination of two very distinct mechanisms at two distinct scales in the tree: the leaves and the branches. Considering the wide range of applications involved in plant science, biology and engineering, it is hoped that our preliminary findings will allow developing new models in these fields.

Appendix A. Material and methods

A.1. Data acquisition

The experiment was carried out in a wind tunnel of test section (5×6 m), at CSTB, Nantes in France. The wind speed was varied step by step from 0.9 to 7.5 m s at the wind tunnel command. For each step, the wind velocity was set for 90 s before we started recording to avoid transient effects on the airflow. The actual wind speed at the tree level was measured by a helix anemometer. Images and drag were recorded for 30 s at each step. The tree was a *Prunus Cerasus*, variety *Hedelfingen giant* of about 3 m high placed at the centre of the wind tunnel test section. It was grown in a pot within a wind-protected area. Its root system is expected to be less extensive than that of a tree grown in nature. The range of moderate wind velocities used in the experiment are far below the wind velocity necessary to uproot a tree, thus the anchorage of the tree is not crucial. Moreover, to assure better anchorage we decided to maintain the basis of the trunk and the pot with additional stiff ropes to avoid

any influence of particular lower mechanical boundary conditions. As such the first mode of the tree (in the sense of [64]) was not found in the response under wind.

Tree motion was recorded by two high-speed cameras. The first camera was a Lumenera Lt225C fitted with a wide angle lens Pentax C30823KP–C814-5M. This camera was monitored with the StreamPix software. USB 3 connection and SSD disks were able to record 160 full HD frames (2048×1080 pix) per second without memory limit. The camera was oriented orthogonally to the airflow to record one side of the tree. Those images were used to compute the foliage velocity V. The second camera was fixed on the ground and oriented upwards. This camera was filming at 250 image per second for 20 s with large resolution (1024×1024 pix). Those images were used to compute the light interception I.

The tree was placed on a six axis load cell at the centre of the test section. Drag was recorded from the load cell using the CSTB wind tunnel facilities for each step at a fixed wind velocity. Before each new drag measurement, the load cell was zeroed.

A.2. Data analysis

For each film corresponding to one wind-velocity step, the sequence of frames was analysed using the KLT-flow option of the CR-toolbox [50] for Matlab (Eulerian tracking method). For each frames, 2000 points with the parameter value *distance* set at 6 were tracked. The toolbox output was the velocity field of the foliage.

For each wind-velocity step, the foliage velocity field was separated into spatio-temporal modes both orthogonal in space and time with the BOD algorithm [68]. The modes in space are 2D velocity fields, called *topos*. At each *topos* is associated a temporal evolution called *chronos*. Examples of such modes are displayed figure 3a. At this step, we discard optical modes with too high-frequency content corresponding to foliage self-overlaying or tracking errors. The rejection criterion is a mean power spectral density (PSD) between 0 and 15 Hz smaller than 1.3 times the mean PSD between 15 and 80 Hz.

Separation between leaves modes L and branch modes B is done through a spatial criterion. If p is the mode perimeter and s is the mode surface onto the *topos* norm map. If $s/p < 1$ cm, the mode belongs to the leaf family. Contrary, if $s/p > 1$ cm, the mode belongs to the branch family.

The light interception is computed with the images of the foliage recorded underneath the tree. Each image is thresholded black and white to separate the foliage from the sky. The instantaneous normalized light interception of the tree is computed as the surface of the foliage (black) divided by the total surface of the picture. This value is averaged over the full image sequence for each step in wind velocity.

Appendix B. Models

B.1. Turbulence buffeting of the branches

We consider a branch as a single-mode structure of mass M and eigen frequency Ω excited by wind turbulence. The branch is immersed in a mean fluid flow that damps its motion. The resulting reduced damping is proportional to the mean wind velocity, U, as $\xi = U\rho S \, C_D/2\Omega M$ [55],

where ρ is the air density, S is the total area of leaves held by the branch, C_D is the drag coefficient of the branch. Considering the resonant response of the branch to the wind turbulence, it is well accepted that the wind turbulence creates a rms displacement Q scales as, [55],

$$Q^2 \propto \frac{\pi (\rho S \, C_D U)^2}{2\xi \Omega^3 M^2 L_b^2} S_u(\Omega), \qquad (\text{B 1})$$

where L_b is the length of the branch and S_u is the power spectral density of the wind velocity fluctuations. In the following, S_u is the von Kàrmàn model of turbulence [57],

$$S_u(\Omega) = \frac{4l_u \sigma_u^2}{U} \frac{1}{(1 + 70.7(\Omega l_u/2\pi U)^2)^{5/6}}, \qquad (\text{B 2})$$

where $l_u \simeq 1$ m, and $\sigma_u/U \simeq 0.1$. For frequencies smaller than 1 Hz, we have $S_u \propto U^{8/3}$ as long as $U < 10$ m s^{-1}. One finds $Q \propto U^{11/6}$.

If all dimensions are scaled by a factor β, we have $S_u \propto \beta^0$, $L_b \propto \beta$, $M \propto \beta^3$, $\Omega \propto D/L^2 \sqrt{E/\rho} \propto \beta^{-1}$ and $S/\xi \propto \Omega M \propto \beta^2$. Finally Q scales as $\beta^{-1/2}$. The velocity of the branches scales as $L_b \Omega Q$ and therefore

$$V_b \propto \beta^{-1/2}. \qquad (\text{B 3})$$

B.2. Leaf flutter

The flutter instability is known to start at different wind velocities depending on leaf orientation and leaf mechanical properties [45]. A simple criterion defines the critical wind velocity for a leaf to flutter,

$$U_c = \frac{40\pi m_s f_l \xi_l}{3\rho \cos\gamma \sin\delta}, \qquad (\text{B 4})$$

where m_s is the surface mass density of the lamina, f_l is the leaf natural frequency in rotation, ξ_l the structural damping of the leaf, ρ the air density and γ and δ two angles defined with the leaf normal vector, the wind direction and the axis of rotation of the leaf. The typical leaf geometrical and mechanical characteristics, table 1, with $\gamma = 0$ and $\delta = \pi/2$, allow computation of the critical wind velocity, $U_c^0 = 1.35$ m s^{-1}.

The fluttering velocity scales as the product of the leaf torsional frequency by the width of the lamina $V_l \propto f_l w_l$. The leaf torsional frequency reads

$$f_l \propto \sqrt{\frac{G t_p^4}{\rho_l L_p w_l^3 L_l t_l}}, \qquad (\text{B 5})$$

where G is the shear modulus of the petiole, ρ_l the density of the leaf, t_p and L_p the thickness and the length of the petiole, t_l, w_l and L_l the thickness, the width and the length of the lamina.

Consider now a different tree, where all dimensions (length, width and thickness) are scaled by a factor β. The level of foliage velocity induced by flutter will scale as $f_l w_l/2$, where f_l is the frequency of torsion of the leaf, and w_l is the width of the lamina. The frequency of the torsion mode essentially depends on the torsional stiffness of the petiole and on the mass of the lamina, the frequency of the mode in torsion would scale as β^{-1}. Therefore, the level of leaf-related foliage velocity would scale as β^0. Similarly, the critical velocity for leaf flutter vary as $U_c \propto \beta^0$ and is also independent of leaf size.

B.3. Reconfiguration threshold

The Cauchy number for leaves may be defined as the ratio of bending moment of the leaf to the elastic response of the petiole

$$C_y = \frac{\rho U^2 \pi L_1^2 w_1 L_P}{8B}, \tag{B 6}$$

where U is the wind velocity, B is the rigidity modulus of the petiole (product of the Young modulus by the second moment of area, for a cherry tree), and is typically $10^{-4}\,\mathrm{kg\,m^3\,s^{-2}}$, [48].

L_P is the length of the petiole, L_1 (respectively, w_1) the length (respectively, the width) of the lamina and ρ the air density. Typical values of mechanical parameters for the cherry tree are gathered in table 1. One computes the regime crossing, $C_y = 1$, where leaves start to deform, for a wind velocity $U = 3.2\,\mathrm{m\,s^{-1}}$.

Again, if we scale all dimensions by an allometric factor β, we have $B \propto \beta^4$, $L_P \propto \beta^1$, $L_1 \propto \beta^1$ and $w_1 \propto \beta^1$. The Cauchy number is not affected by this allometry, $C_y \propto \beta^0$.

References

1. de Langre E. 2008 Effects of wind on plants. *Annu. Rev. Fluid Mech.* **40**, 141–168. (doi:10.1146/annurev.fluid.40.111406.102135)

2. Gardiner B, Berry P, Moulia B. 2016 Wind impacts on plant growth, mechanics and damage. *Plant Sci.* **245**, 94–118. (doi:10.1016/j.plantsci.2016.01.006)

3. Schuepp PH. 1972 Studies of forced-convection heat and mass transfer of fluttering realistic leaf models. *Boundary Layer Meteorol.* **2**, 263–274. (doi:10.1007/BF02184768)

4. Vogel S. 2009 Leaves in the lowest and highest winds: temperature, force and shape. *New Phytologist* **183**, 13–26. (doi:10.1111/j.1469-8137.2009.02854.x)

5. Grace J. 1978 The turbulent boundary layer over a flapping populus leaf. *Plant Cell Environ.* **1**, 35–38. (doi:10.1111/j.1365-3040.1978.tb00743.x)

6. Defraeye T, Herremans E, Verboven P, Carmeliet J, Nicolaï B. 2012 Convective heat and mass exchange at surfaces of horticultural products: a microscale CFD modelling approach. *Agric. For. Meteorol.* **162**, 71–84. (doi:10.1016/j.agrformet.2012.04.010)

7. Burgess AJ, Retkute R, Preston SP, Jensen OE, Pound MP, Pridmore TP, Murchie EH. 2016 The 4-dimensional plant: effects of wind-induced canopy movement on light fluctuations and photosynthesis. *Front. Plant. Sci.* **7**, 1392. (doi:10.3389/fpls.2016.01392)

8. Roden JS. 2003 Modeling the light interception and carbon gain of individual fluttering aspen (*Populus tremuloides* Michx) leaves. *Trees-Struct. Func.* **17**, 117–126. (doi:10.1007/s00468-002-0213-3)

9. Roden JS, Pearcy RW. 1993 Photosynthetic gas exchange response of poplars to steady-state and dynamic light environments. *Oecologia* **93**, 208–214. (doi:10.1007/BF00317673)

10. Roden JS, Pearcy RW. 1993 Effect of leaf flutter on the light environment of poplars. *Oecologia* **93**, 201–207. (doi:10.1007/BF00317672)

11. Moulia B *et al.* 2011 Integrative mechanobiology of growth and architectural development in changing mechanical environments. *Mech. Integr. Plant Cells Plants* **9**, 269–302. (doi:10.1007/978-3-642-19091-9_11)

12. Kuparinen A. 2006 Mechanistic models for wind dispersal. *Trends Plant Sci.* **11**, 296–301. (doi:10.1016/j.tplants.2006.04.006)

13. Timerman D, Greene DF, Urzay J, Ackerman JD. 2014 Turbulence-induced resonance vibrations cause pollen release in wind-pollinated *Plantago lanceolata* L. (Plantaginaceae). *J. R. Soc. Interface* **11**, 20140866. (doi:10.1098/rsif.2014.0866)

14. Stansly PA, Rouse RE, Cromwell RP. 1996 Deposition of spray material on citrus fruit and foliage by air and ground application. *Proc. Florida State Hort. Soc.* **109**, 34–40.

15. Endalew AM, Debaer C, Rutten N, Vercammen J, Delele MA, Ramon H, Nicolaï BM, Verboven P. 2011 Modelling the effect of tree foliage on sprayer airflow in orchards. *Boundary Layer Meteorol.* **138**, 139–162. (doi:10.1007/s10546-010-9544-6)

16. Gilet T, Bourouiba L. 2014 Rain-induced ejection of pathogens from leaves: revisiting the hypothesis of splash-on-filmusing high-speed visualisation. *Integrative Comparative Biol.* **54**, 974–984. (doi:10.1093/icb/icu116)

17. Yamazaki K. 2011 Gone with the wind: trembling leaves may deter herbivory. *Biol. J. Linnean Soc.* **104**, 738–747. (doi:10.1111/j.1095-8312.2011.01776.x)

18. Warren J. 2015 Is wind-mediated passive leaf movement an effective form of herbivore defence? *Plant Ecol. Evol.* **148**, 52–56. (doi:10.5091/plecevo.2015.1042)

19. Hashim MH, Stavrou S. 2006 Measurements and modelling of wind influence on radiowave propagation through vegetation. *IEEE Trans. Wireless Commun.* **5**, 1055–1064. (doi:10.1109/TWC.2006.1633358)

20. Meng YS, Lee YH. 2010 Investigations of foliage effect on modern wireless communication systems: a review. *Prog. Electromagn. Res.* **105**, 313–332. (doi:10.2528/PIER10042605)

21. Roberts AI, Roberts SGB. 2015 Gestural communication and mating tactics in wild chimpanzees. *PLoS ONE* **10**, e0139683. (doi:10.1371/journal.pone.0139683)

22. Peters RA, Hemmi JM, Zeil J. 2007 Signaling against the wind: modifying motion-signal structure in response to increased noise. *Curr. Biol.* **17**, 1231–1234. (doi:10.1016/j.cub.2007.06.035)

23. Shinya M, Fournier A 1992 Stochastic motion—motion under the influence of wind. In *Computer graphics forum*, vol. 11, pp. 119–128. Wiley Online Library.

24. Akagi Y, Kitajima K. 2006 Computer animation of swaying trees based on physical simulation. *Comput. Graph.* **30**, 529–539. (doi:10.1016/j.cag.2006.03.017)

25. Selino A, Jones M. 2013 Large and small eddies matter: animating trees in wind using coarse fluid simulation and synthetic turbulence. In *Computer Graphics Forum*, vol. 32, pp. 75–84. Wiley Online Library.

26. Long J, Porter B, Jones M. 2015 Animation of trees in wind using sparse motion capture data. *Vis. Comput.* **31**, 325–339. (doi:10.1007/s00371-014-0927-4)

27. Raupach MR, StThom A. 1981 Turbulence in and above plant canopies. *Annu. Rev. Fluid Mech.* **13**, 97–129. (doi:10.1146/annurev.fl.13.010181.000525)

28. Sterling M, Baker CJ, Berry PM, Wade A. 2003 An experimental investigation of the lodging of wheat. *Agric. For. Meteorol.* **119**, 149–165. (doi:10.1016/S0168-1923(03)00140-0)

29. Doaré O, Moulia B, de Langre E. 2004 Effect of plant interaction on wind-induced crop motion. *J. Biomech. Eng.* **126**, 146–151. (doi:10.1115/1.1688773)

30. Py C, de Langre E, Moulia B. 2006 A frequency lock-in mechanism in the interaction between wind and crop canopies. *J. Fluid. Mech.* **568**, 425–449. (doi:10.1017/S0022112006002667)

31. Dupont S, Gosselin F, Py C, DeLangre E, Hemon P, Brunet Y. 2010 Modelling waving crops using large-eddy simulation: comparison with experiments and a linear stability analysis. *J. Fluid Mech.* **652**, 5–44. (doi:10.1017/S0022112010000686)

32. Sellier D, Brunet Y, Fourcaud T. 2008 A numerical model of tree aerodynamic response to a turbulent airflow. *Forestry* **81**, 279–297. (doi:10.1093/forestry/cpn024)

33. Sellier D, Fourcaud T. 2009 Crown structure and wood properties: influence on tree sway and response to high winds. *Am. J. Bot.* **96**, 885–896. (doi:10.3732/ajb.0800226)

34. Schindler D, Vogt R, Fugmann H, Rodriguez M, Schönborn J, Mayer H. 2010 Vibration behavior of plantation-grown Scots pine trees in response to wind excitation. *Agric. For. Meteorol.* **150**, 984–993. (doi:10.1016/j.agrformet.2010.03.003)

35. Pivato D, Dupont S, Brunet Y. 2014 A simple tree swaying model for forest motion in windstorm conditions. *Trees* **28**, 281–293. (doi:10.1007/s00468-013-0948-z)

36. Hallé F, Oldeman R. 1970 *Essai sur l'architecture et la dynamique de croissance des arbres tropicaux.* Paris, France: Masson.

37. Milne R. 1991 Dynamics of swaying of *Picea sitchensis. Tree. Physiol.* **9**, 383–399. (doi:10.1093/treephys/9.3.383)

38. Kerzenmacher T, Gardiner B. 1998 A mathematical model to describe the dynamic response of a spruce tree to the wind. *Trees* **12**, 385–394. (doi:10.1007/s004680050165)

39. Rudnicki M, Mitchell SJ, Novak MD. 2004 Wind tunnel measurements of crown streamlining and drag relationships for three conifer species. *Can. J. Forest Res.* **34**, 666–676. (doi:10.1139/x03-233)

40. Moore JR, Maguire DA. 2004 Natural sway frequencies and damping ratios of trees: concepts, review and synthesis of previous studies. *Trees* **18**, 195–203. (doi:10.1007/s00468-003-0295-6)

41. Vollsinger S, Mitchell SJ, Byrne KE, Novak MD, Rudnicki M. 2005 Wind tunnel measurements of crown streamlining and drag relationships for several hardwood species. *Can. J. Forest Res.* **35**, 1238–1249. (doi:10.1139/x05-051)

42. Cao J, Tamura Y, Yoshida A. 2012 Wind tunnel study on aerodynamic characteristics of shrubby specimens of three tree species. *Urban Forestry Urban Greening* **11**, 465–476. (doi:10.1016/j.ufug.2012.05.003)

43. Niklas KJ. 1992 Petiole mechanics, light interception by lamina, and 'economy in design'. *Oecologia* **90**, 518–526. (doi:10.1007/BF01875445)

44. Niklas KJ. 1996 Differences between *Acer saccharum* leaves from open and wind-protected sites. *Ann. Bot.* **78**, 61–66. (doi:10.1006/anbo.1996.0096)

45. Tadrist L, Julio K, Saudreau M, de Langre E. 2015 Leaf flutter by torsional galloping: experiments and model. *J. Fluids Struct.* **56**, 1–10. (doi:10.1016/j.jfluidstructs.2015.04.001)

46. Monsi M, Saeki T. 2005 On the factor light in plant communities and its importance for matter production. *Ann. Bot.* **95**, 549–567. (doi:10.1093/aob/mci052)

47. Pisek J, Sonnentag O, Richardson AD, Mõttus M. 2013 Is the spherical leaf inclination angle distribution a valid assumption for temperate and boreal broadleaf tree species? *Agric. Forest Meteorol.* **169**, 186–194. (doi:10.1016/j.agrformet.2012.10.011)

48. Tadrist L, Saudreau M, deLangre E. 2014 Wind and gravity mechanical effects on leaf inclination angles. *J. Theor. Biol.* **341**, 9–16. (doi:10.1016/j.jtbi.2013.09.025)

49. Py C, de Langre E, Moulia B, Hémon P. 2005 Measurement of wind-induced motion of crop canopies from digital video images. *Agric. For. Meteorol.* **130**, 223–236. (doi:10.1016/j.agrformet.2005.03.008)

50. Diener J, Barbacci A, Hemon P, de Langre E, Moulia M. 2012 Cr–kineplant toolbox. In *Proc. of the 7th Plant Biomechanics Int. Conference, Clermont-Ferrand, France.* Clermont-Ferrand, France: INRA. p. 179.

51. Barbacci A, Diener J, Hémon P, Adam B, Donès N, Reveret L, Moulia B. 2014 A robust videogrametric method for the velocimetry of wind-induced motion in trees. *Agric. Forest Meteorol.* **184**, 220–229. (doi:10.1016/j.agrformet.2013.10.003)

52. Rodriguez M, Ploquin S, Moulia B, de Langre E. 2012 The multimodal dynamics of a walnut tree: experiments and models. *J. Appl. Mech.* **79**, 044505. (doi:10.1115/1.4005553)

53. Der Loughian C, Tadrist L, Allain J-M, Diener J, Moulia B, de Langre E. 2014 Measuring local and global vibration modes in model plants. *C. R. Méc.* **342**, 1–7. (doi:10.1016/j.crme.2013.10.010)

54. Blevins RD. 1984 *Applied fluid dynamics handbook.* 1. New York, NY: Van Nostrand Reinhold Co.

55. Blevins RD. 1977 *Flow-induced vibration*, vol. 1. New York, NY: Van Nostrand Reinhold Co.

56. Païdoussis MP, Price SJ, de Langre E. 2010 *Fluid–structure interactions: cross-flow-induced instabilities.* Cambridge, UK: Cambridge University Press.

57. Hémon P. 2006 *Vibrations des structures couplées avec le vent.* Palaiseau, France: Éditions École Polytechnique.

58. Vogel S. 1989 Drag and reconfiguration of broad leaves in high winds. *J. Exp. Bot.* **40**, 941–948. (doi:10.1093/jxb/40.8.941)

59. de Langre E, Gutierrez A, Cossé J. 2012 On the scaling of drag reduction by reconfiguration in plants. *C. R. Méc.* **340**, 35–40. (doi:10.1016/j.crme.2011.11.005)

60. Harder DL, Speck O, Hurd CL, Speck T. 2004 Reconfiguration as a prerequisite for survival in highly unstable flow-dominated habitats. *J. Plant Growth Regul.* **23**, 98–107. (doi:10.1007/s00344-004-0043-1)

61. Siniscalchi F, Nikora V. 2013 Dynamic reconfiguration of aquatic plants and its interrelations with upstream turbulence and drag forces. *J. Hydraul. Res.* **51**, 46–55. (doi:10.1080/00221686.2012.743486)

62. Alben S, Shelley M, Zhang J. 2002 Drag reduction through self-similar bending of a flexible body. *Nature* **420**, 479–481. (doi:10.1038/nature01232)

63. Gosselin F, de Langre E, Machado-Almeida BA. 2010 Drag reduction of flexible plates by reconfiguration. *J. Fluid Mech.* **650**, 319–341. (doi:10.1017/S0022112009993673)

64. Rodriguez M, de Langre E, Moulia B. 2008 A scaling law for the effects of architecture and allometry on tree vibration modes suggests a biological tuning to modal compartmentalization. *Am. J. Bot.* **95**, 1523–1537. (doi:10.3732/ajb.0800161)

65. Gross G. 1987 A numerical study of the air flow within and around a single tree. *Boundary Layer Meteorol.* **40**, 311–327. (doi:10.1007/BF00116099)

66. Theckes B, De Langre E, Boutillon X. 2011 Damping by branching: a bioinspiration from trees. *Bioinspir. Biomim.* **6**, 046010. (doi:10.1088/1748-3182/6/4/046010)

67. Miller LA, Santhanakrishnan A, Jones S, Hamlet C, Mertens K, Zhu L. 2012 Reconfiguration and the reduction of vortex-induced vibrations in broad leaves. *J. Exp. Biol.* **215**, 2716–2727. (doi:10.1242/jeb.064501)

68. Aubry N, Guyonnet R, Lima R. 1991 Spatiotemporal analysis of complex signals: theory and applications. *J. Stat. Phys.* **64**, 683–739. (doi:10.1007/BF01048312)